Role of Ground Surface Deformation in Volcano Monitoring

5

What can be learned about the inner working of volcanoes by studying how they change shape or deform? What role does InSAR play in volcano deformation studies, and what other techniques are useful for studying deforming volcanoes? By what means and to what extent can volcanic eruptions and their impacts be forecast using deformation and other types of data? In this chapter we address these questions from the perspective of two volcano scientists with very different backgrounds and five decades of combined experience. We conclude that deformation studies alone—no matter how thorough or insightful—cannot provide a "silver bullet" capable of answering all of our questions about volcanoes and how they behave. At the same time, we think that no volcano monitoring system can be considered complete without a vigorous deformation component. The complexities of volcanic systems are too many and varied to be unraveled with any one discipline or technique. However, geodesy as a whole, and InSAR in particular, rank high among the tools that have demonstrated their effectiveness in the past and show considerable promise for the future.

In addition to geodesy, most volcano-monitoring techniques derive from the fields of seismology or geochemistry. The multidisciplinary field of remote sensing also plays an increasingly important role in gas emission studies (Oppenheimer et al. 1998) as well as identification and tracking of volcanic ash plumes that can threaten aircraft (Casadevall 1994; http://gallery.usgs.gov/videos/625). Volcano seismologists use sensitive instruments called geophones to "listen" to various noise sources beneath volcanoes, including (a) volcano-tectonic earthquakes (rock-breaking events sometimes caused by pressurization of a magma body or magma movement) and (b) lower-frequency vibrations that can indicate the presence of magma, gases, or other fluids (Chouet 2003; http://gallery.usgs.gov/videos/605). When magma reaches the surface, distinctive seismic signals indicate the vigor of the eruptive process and can be used to assess the course of the eruption. Emission of magmatic gases is another common manifestation of volcanic activity that can be used to assess the state of a volcano, especially during the precursory phase to an eruption. Geochemical monitoring techniques mostly fall into four broad categories (Sutton et al. 1992): (1) field sampling of fumaroles or thermal springs with subsequent laboratory analyses; (2) measurements of the emission rates of magmatic gases in volcanic plumes; (3) continuous on-site monitoring of the concentrations of selected volcanic gases; and (4) measurements of the concentrations and fluxes of volcanic gases in soils. Measurements of magmatic gas fluxes at volcanoes not only provide important information about the volume and depth of potentially eruptible magma, but also help identify recently active volcanic systems (Sutton and et al. 1992). The remainder of this chapter deals with a third important indicator of volcanic unrest, ground deformation, and the information it can provide about the inner workings of volcanoes in the Aleutians and elsewhere.

5.1 Monitoring Ground Deformation to Aid Eruption Forecasting

Monitoring the changing shapes of volcanoes dates back at least to the first century BCE, although the Roman artisans who built the marble-columned Serapeo market in the coastal town of Pozzuoli—which served as the recording medium—were unwitting volcanologists. The Serapeo has two generations of floors and columns: the second was built after the first sank and was submerged below sea level. This remarkable subsidence is recorded by holes in the market's columns bored by *Lithodomus lithophagus*, a marine mollusk that burrows into rock for shelter. Imagine the consternation of generations of townspeople as the market and its surroundings sank by as much as 11 m from the first

Z. Lu and D. Dzurisin, *InSAR Imaging of Aleutian Volcanoes*,
Springer Praxis Books, DOI: 10.1007/978-3-642-00348-6_5,

century BCE to 1000 CE, at an average rate of about 1 cm/year (Parascandola 1947). And their bewilderment as the columns rose about 2 m from 1000 to 1198, only to be followed by a volcanic eruption at nearby Solfatara Crater (Parascandola 1947; Caputo 1979). Uplift continued to the extent that in 1503 a portion of newly emerged shoreline was deeded to the local university; net uplift during 1000–1538 was about 12 m. The uplift rate accelerated dramatically during several years before an eruption at Monte Nuovo, a new vent in the area, which began on 29 September 1538. The most rapid uplift occurred on 26–27 September, when the ground level at Pozzuoli rose at least 4–5 m in 48 h, causing the shoreline to recede 400 m!

We now realize that Pozzuoli is situated near the center of Campi Flegrei (also known as Phlegraean Fields), a 13-km-wide caldera about 10 km west of Naples. Campi Flegrei is one of the most persistently dynamic calderas on Earth, as evidenced by the remarkable ups and downs recorded in the columns of the Serapeo (Newhall and Dzurisin 1988, pp. 95–117). The residents of Pozzuoli must have realized—at least in hindsight—that rapid emergence of their town from the sea and the incessant earthquakes that surely accompanied the uplift were warning signs of the impending eruption. Today, ground deformation detected near volcanoes serves the same purpose, i.e., as an indicator of volcanic unrest that sometimes leads to an eruption. At Mount St. Helens, for example, a recognizable pattern of increasing seismicity and deformation was the basis for successful predictions of thirteen successive episodes of lava dome growth between June 1980 and December 1982 (Swanson et al. 1983; Dzurisin et al. 1983).

Not in every case is volcano deformation so easy to detect, nor are the implications of ground motion for ensuing eruptive activity so clear. Again, Mount St. Helens provides a good example. On September 23, 2004, two events of significance occurred near the volcano: (1) a swarm of small, shallow earthquakes began that later intensified and culminated with an explosion on October 1, 2004, and extrusion of the first of several lava spines starting on October 11, 2004, and (2) simultaneously, a continuously-recording GPS station at Johnston Ridge Observatory (JRO), 9 km north of the volcano, began to move toward the volcano and downward—indicating that a magma reservoir beneath the volcano was depressurizing (Lisowski et al. 2008). The congruence of those two happenings and the recognition a few days later of a welt growing on the crater floor—all indicating that magma was moving toward the surface—led the USGS–CVO and the Pacific Northwest Seismic Network (PNSN) to issue an Information Statement on September 23, a Notice of Volcanic Unrest on September 26, a Volcano Advisory on September 29, and a Volcano Alert on October 2. The combination of strong seismicity and intense deformation of the crater floor provided clear and increasing warning that an eruption was imminent. The first of four explosions in five days occurred on October 1, 2004, and extrusion of a lava dome starting ten days later continued until early 2008.

But there was a catch. The CGPS station at JRO had been operating since 1997 and had detected no movement upward or away from the volcano right up until the time the earthquakes started and the station began moving down and inward. Upward and outward movement at JRO would be expected if the magma reservoir that fed the 2004–2008 eruption had pressurized or filled with new magma beforehand. What's more, the total amount of inward and downward movement at JRO during the course of the eruption was only about 30 mm, which is difficult to reconcile with the large volume of lava that emerged from the vent (Dzurisin et al. 2008; Mastin et al. 2008). So in this case, the message from ground deformation was ambiguous. On one hand, there was no indication from geodesy that the magma reservoir had pressurized during the 7 years immediately preceding the start of the eruption—even though the CGPS station at JRO was well situated to detect the reservoir *de*pressurizing. Of course, it's possible that the reservoir inflated sometime after the previous period of dome growth ended in 1986 and before the JRO CGPS station was installed in 1997. In fact, Moran (1994) and Moran et al. (2008) concluded from seismic and other evidence that the reservoir repressurized during 1987–1992 and thereafter. Nonetheless, the available geodetic data provide no evidence, even in hindsight, that could have been useful for anticipating the eruption—until an enormous welt started rising on the crater floor just a week before the first explosion on October 1, 2004 (Scott et al. 2008). And in the absence of other information the amount of far-field deformation recorded at JRO would have led to an underestimate of the volume of magma extruded by a factor of 4–5 (Lisowski et al. 2008).

On the other hand, while the JRO deformation record was underwhelming in terms of its usefulness for anticipating the onset and character of the 2004–2008 eruption, intense deformation of the crater floor and Crater Glacier in the near-field was nothing short of spectacular. While JRO was creeping toward the volcano at rates of less than 1 mm/day in late September and early October, parts of the crater floor and glacier were bulging upward 5–10 m/day ($\sim$70 m of height change by October 4) to form a large, fractured welt (Schilling et al. 2008; Vallance et al. 2008)—an unmistakable harbinger of the impending eruption. So in this case ground deformation provided no indication than an eruption was brewing in the long-term or intermediate-term (years to months), but very clear warning in the short-term (weeks to days). Stated differently, no precursory deformation was detected in the far-field (>5 km) as a result of pressurization of the crustal magma reservoir, but dramatic deformation

occurred in the near-field (<1 km from the eventual vent) as a succession of lava spines were thrust to the surface.

Other case studies demonstrate the range of possible insights from ground deformation observations. Contrary to recent experience at Mount St. Helens, subtle far-field deformation sometimes provides the best indicator of an impending eruption. For example, a small network of borehole strainmeters was installed in southern Iceland in 1979 to measure strain changes associated with an expected moderate-size earthquake in the south Iceland seismic zone. The installations were 15–45 km away from Hekla volcano, which was not an intended target for the experiment. Nonetheless, Linde et al. (1993) reported that all of the strainmeters detected extensional strain changes during an explosive eruption at Hekla in January 1991, and the nearest sensor (BUR, 15 km away) showed clear precursory signals starting about 30 min before the eruption began. Linde et al. (1993) successfully modeled the strain changes as a deflating point spherical pressure source (Mogi source, see Sect. 5.3) together with a dike that propagated from a depth of 4 km to the surface. The first anomalous strain signals were simultaneous with the onset of dike propagation, which implies an upward propagation speed of about 8 km/h.

Nine years later, in February 2000, a seismometer that was installed 2 km from the summit of Hekla after its 1991 eruption began to record a swarm of shallow earthquakes, which was unusual for the area. About an hour later, the BUR strainmeter began showing changes that were remarkably similar to those observed just prior to the start of the 1991 eruption—perhaps indicating the ascent of another dike. On that basis, a formal eruption prediction was broadcast to Civil Aviation authorities and the public just a few minutes later (Agustsson et al. 2000). The predicted eruption began about 20 min after the warning was issued and about 90 min after the beginning of the earthquake swarm. This remarkable success story stands as the most specific short-term eruption prediction to date anywhere in the world and argues for more investment in high-precision monitoring instruments near hazardous volcanoes. It is important to note, however, that the successful Hekla prediction in 2000 was possible only because the strain changes closely repeated a pattern that had been seen prior to the 1991 eruption (Roeloffs and Linde 2007, pp. 318–320). Recognition of a recurring pattern of ground deformation or some other eruption indicator can be a powerful prediction tool in some instances, as was the case at Mount St. Helens for dome-building episodes during 1980–1982 (Swanson et al. 1983; Dzurisin et al. 1983), but that approach is not generally applicable to other volcanic crises. Physics-based models that can provide insights into the processes causing ground deformation or other indicators of unrest are preferable, as long as they are firmly based on observational data.

Many other examples of precursory deformation at volcanoes could be cited, some supportive of geodesy as a useful tool for eruption prediction and others not. A wealth of experience around the world shows that most eruptions are unique in some way and therefore hazards assessments and forecasts must be tailored to each specific case. There are differences in tectonic setting, magma composition, eruption interval, location and volume of magma storage, eruption style, number and types of monitoring instruments deployed, availability and involvement of groundwater, surface water, or ice, and many other parameters that affect the style and extent of precursory ground deformation that can be recorded. Given the complexities of volcanic systems and limitations of any single monitoring technique, Dzurisin (2000, p. 1564) concluded "…to distinguish among the full range of possible [deformation] source locations and geometries, especially if multiple sources might be present, it is necessary to make [geodetic] measurements virtually 'everywhere, all the time'". In today's world, that means operating a dense and extensive network of CGPS instruments, strainmeters, or tiltmeters, with real-time data processing and analysis, plus making complementary InSAR and campaign-style GPS observations—both in times of crisis and quiescence. That's a tall but necessary order for all of Earth's most dangerous volcanoes.

5.2 Modeling Deformation Data to Infer Characteristics of Magma Reservoirs

Among the most important parameters needed to assess short-term volcano hazards are the location, volume, and composition of potentially eruptible magma. Together with seismology and gas geochemistry, geodesy helps to constrain these unknowns. Seismic tomography can provide estimates of the total volume of a magma reservoir and the degree of partial melting within it (for example, Husen et al. 2004). Measurements of the emission rates of magmatic volatiles, especially CO_2, can be used to estimate the volume of recently degassed magma beneath a volcano (for example, Gerlach et al. 2002). Models of ground deformation data can be used to identify the location, shape, and pressure change within a magma reservoir. Geologic studies of past eruptive products can provide clues to probable eruption scenarios, including eruptive style, volume, and composition. Each technique has advantages and drawbacks; together they can be used to develop a general idea of the amount, state, and eruptive potential of magma beneath a volcano.

Deformation specialists approach this problem by attempting to minimize the misfit between a deformation data set (for example, a set of station displacements from GPS observations or a deformation interferogram) and a numerical model of the deformation source. The model is characterized by a set of parameters that typically includes the source location (x, y), depth (z), one or more shape factors (for example, the aspect ratio for an ellipsoid), and some measure of source "strength" (pressure change or volume change, see below). Many modelers make the simplifying assumption that the Earth is a uniform elastic half-space, which turns out to be a reasonable approximation under most conditions. In that case, a set of elastic constants uniquely relate the pressure change or volume change at the source to the resulting surface deformation field. Japanese seismologist Kiyoo Mogi was the first to recognize that geodetically-measured surface displacements associated with eruptions in Japan and Hawaii resulted from inflation or deflation of magma reservoirs beneath volcanoes (Mogi 1958). He presented simple mathematical expressions that relate surface displacements to inflation or deflation of a small sphere deeply buried in an elastic half-space (sometimes referred to as a point source of dilatation).[1] Analytical expressions for several other source shapes that are relevant for volcano modeling (for example, ellipsoid, pipe, dike or sill) have been published more recently, but the Mogi model still is the best known and most widely used formulation for modeling surface deformation caused by inflation or deflation of magma reservoirs. Under some circumstances, a viscoelastic medium is more realistic and can be used instead of an elastic one. This introduces time dependence in the deformation field that can provide useful information if time-series deformation data are available for comparison.

When a numerical source model with *a priori* fixed parameters and assumptions is used to predict the resulting surface deformation field, the procedure is called forward modeling. This can be useful for designing a geodetic network, initial comparison to a deformation data set, or selecting the most appropriate source type (for example, Mogi, ellipsoid, pipe, or dike) to use for a more thorough analysis. In the latter case, once a starting model is selected, the model parameters can be adjusted iteratively to achieve the best possible fit between model results and observations; the procedure is called numerical inversion. If more than one type of data are used to constrain the model, the procedure is referred to as simultaneous inversion. In either case, various strategies are available to increase the likelihood that the inversion will settle on the best possible combination of parameters, rather than getting sidetracked and caught in a suboptimal solution (i.e., a local minimum in solution space). An accurate representation of errors in the data, preferably in the form of a full covariance matrix, is essential to properly weight the data and to express realistic uncertainties in best-fit model parameters. The more detailed and accurate the observations are, the better constrained the model will be. Of course, given enough model parameters to adjust, or the flexibility to include multiple deformation sources, it is possible to fit any data set(s) arbitrarily well. The challenge is to arrive at the simplest deformation source model that: (1) fits the data adequately, given the uncertainty inherent in the data and the oversimplifications inherent in the model; (2) is consistent with constraints provided by seismology, gas geochemistry, petrology, and other disciplines; and (3) makes sense from a volcanological perspective. For a detailed discussion of analytical volcano deformation source models, see Lisowski (2007).

A well constrained deformation source model can provide information about the location, depth, shape, and pressure change within a magma reservoir. Source depth is especially important for assessing near-term volcanic hazards. Although there are documented cases of magma ascending from deep within the crust (>10 km) to the surface in a matter of hours to days, in general the shallower the source the greater the concern. This is especially true if the deformation source appears to be moving closer to the surface over time.

The amount of surface displacement that a source at a given depth will produce at a given location depends on the shape of the source. What this means in practical terms is that, with a limited deformation data set, it might be difficult to distinguish between a shallow spheroidal source and a deeper sill or pipe, for example (Lisowski 2007). The deeper the deformation source, the more difficult it is to ascertain its shape from surface displacement data. This is a consequence of the way potential fields behave, as described in mathematical terms by Stokes' Theorem. Simply stated, short-wavelength features of a potential field are more strongly attenuated with distance than long-wavelength features. Imagine a deformation source with a complicated shape at some depth below the surface. Near the source, the deformation field has both short- and long-wavelength characteristics that would allow us to infer the shape of the source very accurately. As we move away from the source and toward the surface (the process is called upward continuation by mathematicians and potential-field

[1] Mogi (1958) presented a mathematical model that now bears his name (the famous "Mogi model" in the vernacular of volcanology), even though Mogi attributed its derivation to Yamakawa (1955). An interesting historical note is that the equations governing the model had been independently derived at least twice before—by Anderson (1936) who applied them to the formation of cone sheets, ring dikes, and cauldron subsidences, and by McCann and Wilts (1951) who used them to analyze ground subsidence caused by oil extraction in the Long Beach–San Pedro area of California.

geophysicists), short-wavelength features that are diagnostic of the source's complexity attenuate faster than long-wavelength features. The latter are indicative of the source's depth and overall shape, but not the details of its shape. As a consequence, all sources below about 10 km depth look about the same from the surface, i.e., they look like a Mogi source. Hence the popularity of that formulation. At shallower depths, however, distinctive features of the deformation fields produced by sources of different shapes begin to emerge. A vertical ellipsoidal source produces slightly less vertical displacement and slightly more horizontal displacement in the near field than a comparable spherical source. Similarly, a sill source (horizontal dislocation) produces more vertical displacement and less horizontal displacement than a comparable dike source (vertical dislocation). With a sufficiently dense and accurate set of surface deformation data, it is possible to characterize the shapes of one or more deformation sources beneath a volcano and thus to study its magma storage and transport system (see Sect. 5.3).

If the mechanical properties of rock hosting a magma reservoir are known (from drilling or geophysical investigations, for example) or assumed, a model-derived pressure change can be converted to an equivalent volume change in the reservoir. That value is a reasonable proxy for the volume of magma added to or withdrawn from the reservoir to produce the observed surface deformation.[2] Large reservoir inflation suggests the potential for a large eruption; large deflation usually accompanies a large eruption or intrusion—but complications can arise. Unfortunately, the interpretation of model results in terms of eruption potential is subject to at least two serious shortcomings. First, magma is a compressible fluid and its compressibility can range over several orders of magnitude depending on gas content, bubble density, crystal fraction, and other factors. Likewise, the reservoir host rock can vary in stiffness (shear modulus). This means that the relationship between the amount of magma added to or withdrawn from a reservoir and the resulting amount of surface deformation can vary widely. Addition of highly compressible magma to a strong reservoir might produce little or no surface deformation, whereas the same amount of nearly incompressible magma added to a weak reservoir would cause much more. Precise gravity measurements, which are sensitive to changes in subsurface mass instead of volume, are the best means to resolve this ambiguity.[3]

A second shortcoming of deformation models is that, even if the volume of magma added to or withdrawn from a reservoir were known accurately, that value is not a direct indicator of the volume or composition of potentially eruptible magma. This is because deformation measurements are inherently differential: they provide information only about incremental changes in the source, not about the magnitude or nature of the source itself. All else being equal, 10 million cubic meters of "new" magma added to a reservoir containing 10 cubic kilometers of "old" magma will produce the same surface deformation field as the same amount of magma added to a much larger (or smaller) reservoir. But the total volume of potentially eruptible magma might vary tremendously among those scenarios. Likewise, adding basalt to a basaltic reservoir will produce the same surface deformation field as adding the same amount of basalt to a rhyolitic reservoir—possibly with vastly different outcomes. Seismic tomography and gas geochemistry are better suited to address these important issues. Combining insights gained from those disciplines with others from geology and geodesy is the most effective means to arrive at a realistic understanding of real-world magma reservoirs.

In summary, numerical models of deformation sources based on surface deformation measurements can provide useful insights into the location, depth, shape, and changing conditions of magma reservoirs and conduits—but they are subject to large uncertainties resulting from imperfect knowledge of the deformation field and of the mechanical and rheological properties of the crust and magma bodies beneath volcanoes. The denser the deformation measurements are in space and time, the more accurate the source model is likely to be. In general, a better Earth model makes possible a better deformation source model.

5.3 Using Deformation Source Models to Study Magmatic Plumbing Systems

Volcanoes and their underpinnings can be thought of as natural mass transit systems, i.e., they facilitate the ascent of magma from a production zone in Earth's mantle or lower crust toward the surface by way of a system of conduits and reservoirs that collectively form a magma transport system. In the preceding section, we discussed the role that deformation source modeling can play in constraining the size,

[2] The relationship between a change in reservoir volume and the corresponding amount of magma added to or withdrawn from the reservoir depends on the compressibility of the magma. For a given change in reservoir volume, much more highly compressible, gas-rich magma can be added or withdrawn than is the case for less compressible, gas-poor magma. In practice, magma compressibility is seldom well constrained, so a model-derived change in reservoir volume is used to approximate the amount of magma added or withdrawn.

[3] Gravity measurements are sensitive to both subsurface mass changes and surface height changes. Simultaneous measurements of gravity and surface height can be used to estimate mass changes in a magma reservoir over time (e.g., Battaglia et al. 2008).

shape, and location of an inferred magma reservoir. Here we expand our scope to the entire magma plumbing system beneath a volcano, which in most cases comprises interconnected conduits and reservoirs that interact with each other, with a deep magma source region, and with the prevailing stress field to produce the activity we observe at the surface. In practice our geodetic tools seldom allow us to "see" more than about 10 km beneath the surface. At greater depths the image is likely to be nondescript because the amount of surface deformation caused by deeper sources is exceedingly small and the mechanical properties of the source region are poorly known. Nonetheless, experience shows that much can be inferred about a volcano's magma plumbing system by combining information gleaned from geodesy, seismology, petrology, and eruptive history—as illustrated by the following two case studies.

5.3.1 Mount St. Helens, Washington

Prior to the 1980 eruption of Mount St. Helens—the first at this young Cascade volcano in 123 years—very little was known about the volcano's magma storage and transport system or about the types of precursors to be expected before eruptive activity resumed. Only one seismometer was operating within 50 km of the volcano: station SHW had been installed on the west flank in 1972 as part of a skeletal USGS volcano monitoring program (Malone et al. 1981). Deformation monitoring also was minimal. A network of benchmarks for EDM measurements had been established at the volcano in 1972, but only one radial 7.6-km line from that network (Smith Creek Butte–East Dome) could be recovered before or after the May 18, 1980, eruption. Changes along that line were within expected measurement error, which—together with null results for other lines established after unrest began in March 1980—indicated that deformation of the edifice and surroundings prior to the May 18 eruption was minimal except for the now-famous bulge on the north flank (Lipman et al. 1981, p. 151). In three decades since the 1980 eruption, much has been learned about the magma plumbing system at Mount St. Helens. The following four sections are arranged chronologically and describe the evolution of thought concerning the magmatic system beneath Mount St. Helens since 1980.

5.3.1.1 March–October 1980: Precursory Unrest and Explosive Eruptions

At 3:47 p.m. PST on March 20, 1980, a *M* 4.2 earthquake shook snow-clad Mount St. Helens in southwest Washington State. It was among the first of countless shocks during the next eight weeks that accompanied the intrusion of a dacite cryptodome and growth of an ominous bulge on the volcano's north flank. Gravitational failure of the distended north flank on May 18 cut the pressurized cryptodome in two, producing one of the largest debris avalanches in historical time and triggering a lateral explosion that devastated 600 km^2 of forest to the west, north, and east. Within minutes, a vertically-directed Plinian eruption column rose to a height of more than 20 km above the vent, and large pyroclastic flows started pouring out of the crater a few hours later. Tephra drifting downwind produced daytime darkness for more than 200 km and visible ashfall as far as 1500 km away. Smaller explosive eruptions and pyroclastic flows occurred in 1980 on May 25, June 12, July 22, August 7, and October 16–18. Small dacite lava domes were emplaced in the vent area during the waning stages of the eruptions in June, August, and October, but the first two were mostly destroyed by subsequent explosions (Christiansen and Peterson 1981). The October 1980 dome survived as the core of the long-lived 1980s dome, which emerged during a series of exogenous and endogenous growth episodes that ended in October 1986 (Swanson et al. 1987).

The 1980–1986 eruptions at Mount St. Helens provided the first opportunity for scientists to study the volcano in action, and much was learned as a result.[4] It came as a surprise that most of the earthquakes that occurred beneath the volcano during March 20–May 17, 1980, were shallow, i.e., within 3 km of the surface (Endo et al. 1981). Following a quiescent period of 123 years since the end of the previous eruptive episode in 1857, some deeper seismicity and upward migration of earthquakes might have been expected as magma intruded toward the surface. However, only a few earthquakes were located as deep as 6-7 km beneath the surface, and no upward migration was detected. Likewise, it seemed reasonable to expect some far-field surface deformation to occur if a magma reservoir beneath the volcano was pressurizing during the two-month period of precursory seismicity. Instead, various types of geodetic observations indicated that measurable deformation was restricted to an area about 1.5 km by 2.0 km in size on the volcano's bulging north flank, where deformation was extreme (Lipman et al. 1981). When studies of the May 18 debris avalanche revealed that it contained fragments of the cryptodome that had intruded the volcano's north flank during the preceding weeks, a startling conclusion became inescapable: magma had risen to within a few hundred meters of the surface

[4] Many of the USGS scientists who responded to the 1980 eruption at Mount St. Helens had previous experience at the Hawaiian Volcano Observatory (HVO), but for most of them Mount St. Helens was their first exposure to an active stratovolcano. Faced with a new set of circumstances, they both imported tried-and-true monitoring techniques from Hawaii and also developed new ones to fit the situation (Ewert and Swanson, 1992).

without causing many earthquakes deeper than ~3 km or measurably deforming the surface beyond a ~3 km^2 area on the north flank. Clearly, a magma conduit of some sort existed in the shallow subsurface beneath the vent area. But what was the nature of the conduit? Did it extend uninterrupted to a magma source in the lower crust–upper mantle, or were there intervening magma reservoirs in the crust? If the latter, what were the depth(s), shape(s), and size(s) of the reservoir(s)? The first clue to the configuration of the deeper magma plumbing system came from seismicity that began soon after the climactic events of May 18, 1980.

Weaver et al. (1981, p. 109) reported that seismicity near Mount St. Helens immediately after the May 18, 1980, eruption differed markedly from that during the preceding two months of precursory activity:

> The seismic sequence that started on March 20 (and produced a combined total seismic energy equivalent to a minimum of a magnitude-6.0 earthquake) was confined to a small volume in the shallow crust directly beneath the north side of the volcano… In marked contrast, earthquakes after the May 18 eruption occurred beneath the volcano at depths down to 20 km, and within several weeks following that eruption, earthquakes were occurring at distances 35 km north and 20 km south of Mount St. Helens.

The post-May 18 seismicity illuminated a much larger volume beneath and around the volcano, and thus gave scientists a glimpse into the mid-crustal magma storage system at Mount St. Helens and the relationship between regional tectonism and volcanism. Weaver and Smith (1983) identified a linear, seismically active zone that extends from 60 km north of Mount St. Helens to 30 km south, and from near the surface to 30 km depth. They dubbed the feature the St. Helens seismic zone (SHZ), judged it capable of generating a moderate- to large-magnitude shallow earthquake, and interpreted focal mechanism data as evidence for locked subduction along the Juan de Fuca-North American plate interface. According to their model, compressive stress accumulation across the locked segment of the plate interface produces strike-slip motion along the NNW-trending SHZ. The SHZ passes directly beneath Mount St. Helens, suggesting that regional tectonics played a role in its emergence. Scandone and Malone (1985, p. 260) analyzed post-May 18 seismicity beneath Mount St. Helens and identified a vertically elongated earthquake-free zone beneath the volcano, which they interpreted as evidence for a magma body:

> We hypothesize a deep reservoir (7–9 km) connected to the surface by a conduit of ~50 m radius. The magma reservoir has dimensions of the order of 10–20 km^3. Withdrawal of magma from this reservoir causes a collapse of the surrounding rocks with associated seismic activity and subsidence of the volcano…. We find no evidence for a shallow magma reservoir of any significant size.

The magmatic underpinnings of Mount St. Helens were starting to come into focus. The following six years of intermittent lava-dome growth helped to sketch in more of the details.

5.3.1.2 October 1980–October 1986: Episodic Lava-Dome Growth

Small dacite lava domes were emplaced during the waning stages of explosive eruptions at Mount St. Helens in June 1980, August 1980, and October 1980. The June and August domes were mostly destroyed by explosive eruptions in July and October, respectively. The October 1980 dome survived and forms the core of the composite dome that grew episodically until October 1986 (Swanson et al. 1987). The onsets of more than a dozen dome-building episodes during that period were predicted successfully from tens of minutes to three weeks in advance, based on a recurring pattern of seismicity and ground deformation that provided additional insights into the shallow magma plumbing system (Swanson et al. 1983).

From December 1980 to October 1986, each of 16 extrusion episodes that lasted from several days to almost a year added from 1×10^6 to 22×10^6 m^3 of dacite lava to the growing dome (Brantley and Myers 2000). Most of the seismicity during this period occurred within about 3 km of the surface, with the exception of a swarm of small, deep earthquakes that preceded an explosive eruption in March 1982 (Weaver et al. 1983). Both shallow seismicity and deformation of the crater floor and dome increased markedly starting several days to a few weeks before extrusion began. Evidence of intense deformation included development of radial cracks and circumferential thrust faults on the crater floor surrounding the dome (Fig. 5.1), contraction of EDM lines from points on the floor to points on the dome, and extension of lines on the dome itself. Measurable deformation did not extend more than about 1 km from the vent, which suggested that the source was very shallow (Swanson et al. 1983). Modeling of the deformation data by Chadwick et al. (1983, 1988) suggested that the 1980–1986 dome-building eruptions were fed from a subsidiary reservoir 2–3 km beneath the crater floor, presumably from a remnant magma body that fed the 1980 intrusion and eruptions. In support of this model, Cashman (1988) measured crystal size distributions in samples of 1980–1986 dome dacite and concluded that continuous groundmass crystallization at a depth consistent with the results of Chadwick et al. (1983, 1988) might have driven episodic extrusion through repeated volatile saturation of the remaining reservoir melt. Ideas about the upper part of Mount St. Helens' magma plumbing system had begun to crystallize as well.

Fig. 5.1 Scientists measure displacement across a radial crack (*top*) and circumferential thrust fault (*bottom*) on the crater floor at Mount St. Helens. USGS photographs taken by Lyn Topinka on 12 May 1984 and by Terry A. Leighley in 1981, respectively

5.3.1.3 1987–2003: Eruptive Quiescence Sets the Stage for Renewed Eruptive Activity

The next important advance in understanding the configuration of Mount St. Helens' magma system was made by Moran (1994), who studied seismicity at the volcano during the non-eruptive period from 1987 to 1992. He noted that earthquakes in the 3–10 km depth range, which were mostly absent during the 1980–1986 period of dome growth, started to occur again several months after the final growth episode in October 1986. By the end of 1989, hypocenters extended from the surface down to 10 km, and between 1987 and mid-1990 the majority were deeper than 4 km (Figs. 5.2 and 5.3). Hypocentral distributions together with stress field modeling suggested that post-May 18 earthquakes during 1980 occurred in response to a pressure drop in an aseismic zone at 7–11 km depth, whereas the 1987–1992 seismicity occurred in response to a pressure increase in an aseismic zone at 6.5–10 km depth. Following earlier workers including Scandone and Malone (1985), Moran (1994) interpreted the aseismic zone as a magma reservoir that fed the 1980 eruptions and he suggested that repressurization of the reservoir occurred as a result of sealing and gas accumulation in the shallow magma conduit. Consistent with that interpretation, line lengths in a regional GPS trilateration network extended slightly from 1982 to 1991, but showed no significant changes from 1991 to 2000 (Lisowski et al. 2008). Moran's (1994) sketch of the magma plumbing system beneath Mount St. Helens (Fig. 5.4) was the most detailed and best constrained effort to date. A lack of measureable ground deformation at Mount St. Helens after dome growth ended in 1986 prevented geodesy from contributing to the picture. Additional

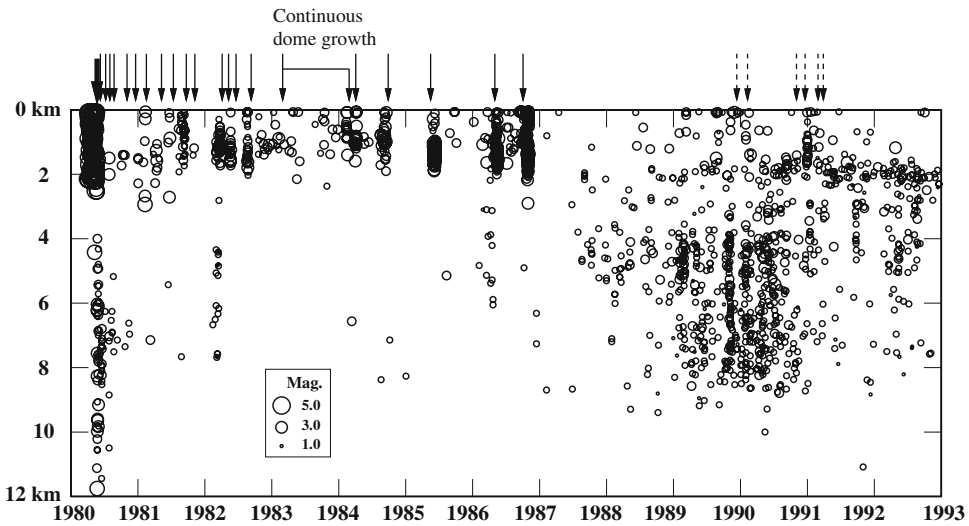

Fig. 5.2 Time-versus-depth plot of all recorded earthquakes that occurred at Mount St. Helens between 1980 and 1992. Time begins on January 1, 1980 and ends on December 31, 1992. *Solid arrows* indicate the onset times of confirmed magmatic eruptions. *Dashed arrows* between 1989 and 1991 correspond to six confirmed steam explosions. Note that 0 km corresponds to mean seismic station elevation, which is about 1 km above sea level at Mount St. Helens. Figure modified slightly from Moran (1994, p. 4342)

details had to await future eruptive activity at the volcano, which began a decade after Moran's study was published.

5.3.1.4 2004–2008: Continuous Lava-Dome Growth by Extrusion of Recumbent Spines

A swarm of shallow (depth < 2 km) earthquakes beneath the 1980 crater at Mount St. Helens began on September 23, 2004, and intensified rapidly following a brief decline on September 25 (Moran et al. 2008). Concurrently with the start of the swarm, CGPS station JRO1 located about 9 km to the north-northwest began moving down and toward the volcano at an initial rate of about 0.5 mm/d. This was the first movement of the station caused by a volcanic process since the station was installed in mid-1997; its earlier movements had been related to regional tectonic processes or local effects such as loading by rime ice during Pacific Northwest winters (Lisowski et al. 2008). The first of four brief explosions occurred on October 1 during a vent-clearing phase, and dacite lava first appeared at the surface on October 11 (Scott et al. 2008). Pre-eruptive seismicity during September–October 2004 was accompanied by spectacular ground deformation. Intense localized uplift formed a welt on the crater floor south of the 1980–1986 dome that, by October 11, grew to 425 m in width, 475 m in length, and 105 m in height with a volume of about 10^7 m^3 (Schilling et al. 2008). Continuous extrusion of a series of recumbent spines during the ensuing 4 years produced a lava dome similar in volume ($\sim 9 \times 10^7$ m^3) to the 1980–1986 dome.

The 2004–2008 eruption gave scientists another opportunity to refine their concepts of the magma plumbing system beneath Mount St. Helens, and although some details remain fuzzy there is general consensus about the system's main elements between the surface and about 15 km depth. The current model is similar in many respects to the ones proposed by Scandone and Malone (1985) and Pallister et al. (1992) based on analyses of the 1980–1986 eruptions. Pallister et al. (2008, pp. 680–681) presented a refined version of the model that incorporates seismic, petrologic, and deformation observations from the 2004–2008 eruption (Fig. 5.5). They drew a vertically elongate magma reservoir extending from about 13 km to 5 km depth beneath the crater floor. The reservoir must be fed episodically by intrusions of dacite from the lower crust or of basalt from the mantle wedge, but at those depths our image of the plumbing system fades to black. Evidence that phenocrysts in the dome dacite formed over wide ranges in temperature and depth is interpreted to mean that convection occurs throughout the reservoir, except in a crystal-rich mush zone near the top. The 1980 eruptions were sourced in the convecting part of the reservoir at 8–9 km depth and the 2004–2008 eruption was sourced in the crystal mush zone at about 5 km depth.

In a more recent paper, Waite and Moran (2009) used local earthquake tomography to image the shallow magmatic system beneath Mount St. Helens. Their results were consistent with those from previous studies, including the existence of an asesimic zone between about 5.5 km depth and at least 8 km depth, which corresponds to the magma reservoir envisioned by earlier workers. In addition, Waite and Moran (2009) detected a seismic low-velocity zone directly beneath the volcano and between about 2 km and 3.5 km BSL (4-5.5 km beneath the crater floor), which they

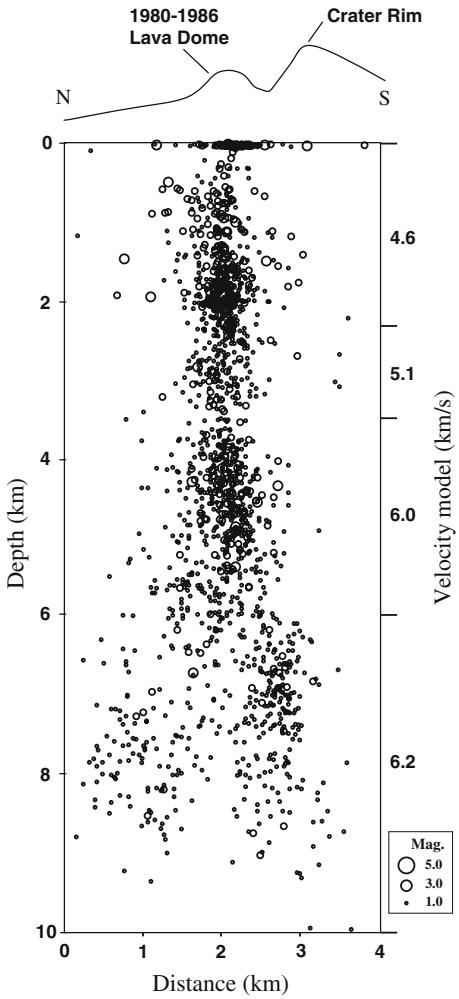

Fig. 5.3 North–south cross-section of seismicity at Mount St. Helens between 1987 and 1992. Note that 0 km on *left axis* corresponds to mean seismic station elevation, which is about 1 km above sea level at Mount St. Helens. *Short horizontal lines* along *right axis* correspond to layer boundaries in the one-dimensional velocity model used to locate the earthquakes (velocities in km/s). Hypocenters are within ±2 km perpendicular distance to N–S plane. Figure modified slightly from Moran (1994, p. 4343))

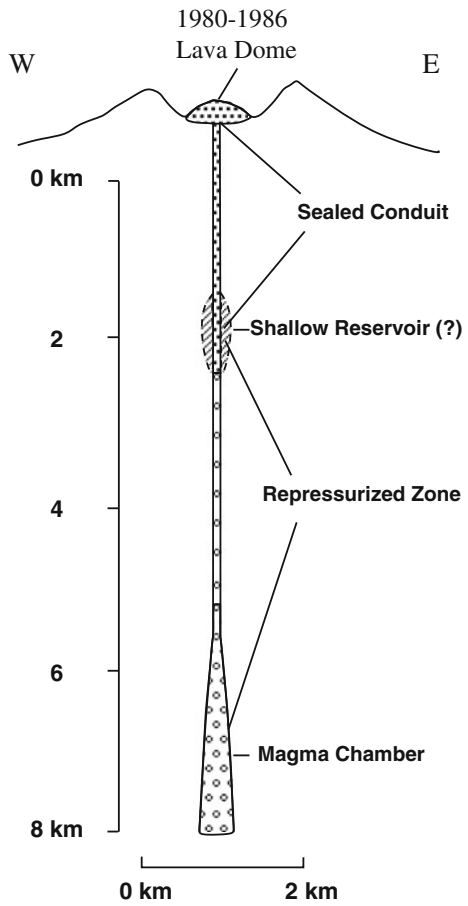

Fig. 5.4 Schematic model of the Mount St. Helens magmatic system. Figure modified slightly from Moran (1994, p. 4353)

interpreted as a shallow magma storage zone. The feature is reminiscent of the shallow reservoir proposed by Chadwick et al. (1983, 1988) as the source of the 1980-1986 dome-building eruptions.

Geodetic studies during 2004–2008 contributed substantially to our understanding of the magmatic system at Mount St. Helens, principally by helping to constrain the location and shape of the crustal reservoir and by providing insight into the nature of the shallow conduit system. Lisowski et al. (2008) modeled far-field deformation data obtained from CGPS stations during the first two years of the 2004–2008 eruption and concluded that the best-fitting source is a near-vertical prolate spheroidal cavity with an aspect ratio of 2:3 embedded in an elastic half-space and centered at 7–8 km depth.[5] This location corresponds reasonably well to the source of the 1980 eruptions proposed by Scandone and Malone (1985), Moran (1994), and Pallister et al. (2008). It is not inconsistent with the shallower (about 5 km depth) source for the 2004–2008 eruption proposed by Pallister et al. (2008) if we assume that the reservoir is centered at 7.5 km depth and the 2004–2008 eruption was fed from the top. In that case, the vertical radius b of the reservoir is 2.5 km and the horizontal radius a is 1.65 km ($a/b = 0.66$). The corresponding reservoir volume $V = \frac{4\pi}{3}a^2b$ is 28.5 km^3, which is about an order of magnitude greater than the largest tephra deposit at Mount St. Helens (see below).

In other studies, Mastin et al. (2008) used geodetic observations and measurements of lava extrusion rate as a function of time to constrain various characteristics of the

[5] The reference level for deformation source depths at Mount St. Helens mentioned here varies by up to ∼2 km. Most are relative to the crater floor at ∼2 km elevation, some are relative to the average elevation of stations in the regional seismic network (∼1 km), and some are relative to sea level. Interested readers might want to consult the original literature cited here for more information.

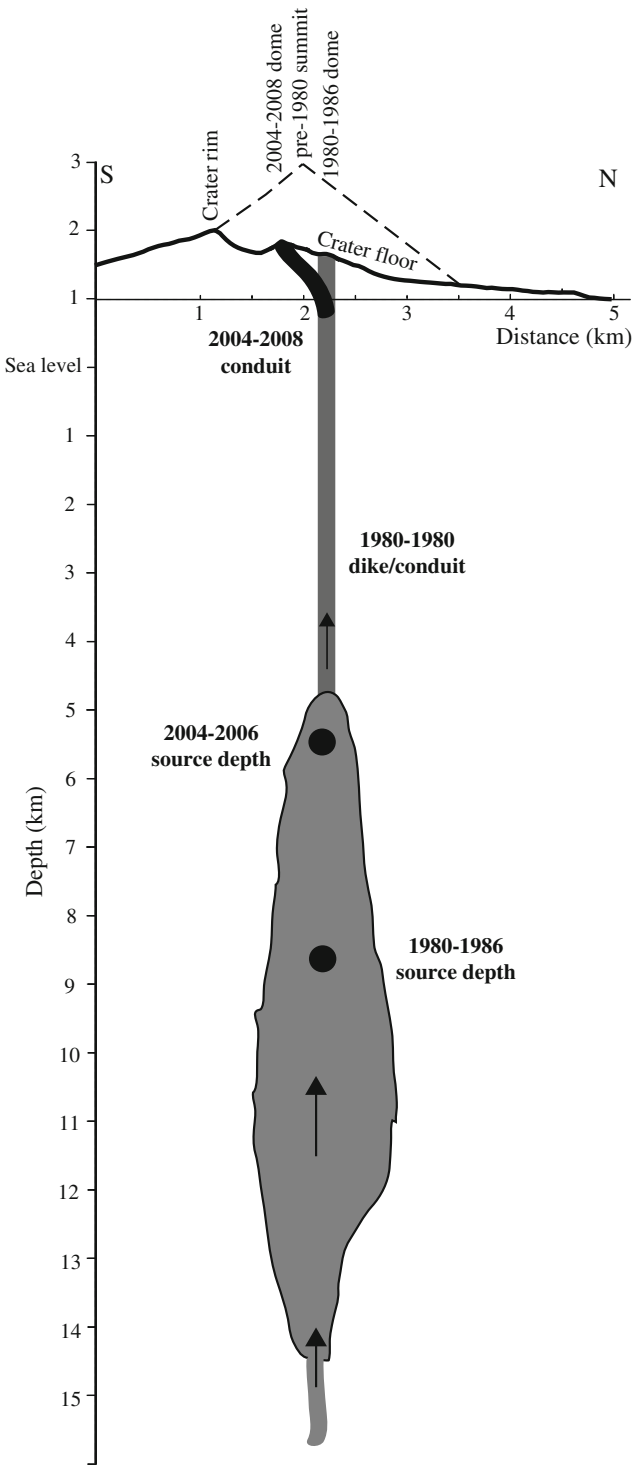

Fig. 5.5 Schematic cross-section of Mount St. Helens plumbing system for 1980–1986 and 2004–2008 eruptions. Diagram is modified from Pallister et al. (2008, p. 681)

Mount St. Helens magma system, including reservoir volume. Their results depend on the assumed values for several parameters that are poorly constrained (e.g., reservoir compressibility, magma compressibility, initial reservoir overpressure, and pressure drop during the eruption). Combinations of model parameters that produce reasonable fits to the data include reservoir volumes in the range 6–24 km^3 (Mastin et al. 2008, p. 478). The middle of that range is a few times larger than the volume of magma erupted during the largest Holocene eruption at Mount St. Helens, i.e., the 3.4 ka Yn eruption that produced 4 km^3 dense-rock-equivalent of dacitic tephra (Mullineaux 1996). The upper end of the range is comparable to the value of 28.5 km^3 for a prolate spheroidal reservoir that is consistent with both geodetic and petrologic constraints imposed by the 2004–2008 eruption (see above). Assuming the largest eruptions do not completely empty the reservoir and recognizing the considerable uncertainty associated with all of the estimates, including unmodeled complexities of the real Earth, we judge the consensus view embodied in Fig. 5.5 to be credible as the prevailing model—an impressive achievement given the inscrutable nature of the deep subsurface.

Geodetic studies also contributed to current understanding of Mount St. Helens' magma plumbing system by providing insight into the mechanical properties of the shallow conduit system and its connection to the underlying reservoir. Both in 1980 and 2004, eruptions were heralded by the appearance of a localized bulge or welt on the volcano very soon after the onset of shallow seismicity. In neither case was this extreme form of surface deformation preceded by more than a small amount of more widespread, deeper-seated deformation resulting from pressurization of the reservoir centered at 7–9 km depth. This suggests that a common assumption made by modelers, i.e., that the crust beneath volcanoes can be represented adequately by a uniform elastic half-space, is not always appropriate at Mount St. Helens. Instead it seems that the upper part of the conduit becomes plugged between eruptive episodes, as was the case prior to 1980 and during 1986–2004. At such times, pressurization of the reservoir as a result of crystallization and fluid exsolution/expansion ("second boiling") or intrusion of magma from below causes deep (3–10 km depth) seismicity of the sort described by Moran (1994) and Moran et al. (2008) for the period 1987–1998, and small amounts of surface dilation as noted by Lisowski et al. (2008) for 1982–1991. Under these conditions the uniform elastic assumption is probably valid. On the other hand, the relative paucity of earthquakes in the 3–10 km depth range during 1998–2004 and the absence of measurable deep-seated deformation during 1991 to 2000—soon followed by intense shallow-seated deformation (growth of the welt on the crater floor during September–October 2004) and extrusion of the 2004–2008 dome—require a more complicated model.

Did pressurization of the reservoir cease sometime during the 1990s and, if so, why did the volcano erupt in 2004? If pressurization continued unabated, why were there fewer

earthquakes below 3 km depth and no measurable far-field deformation after 1998? What are the implications for future activity at Mount St. Helens, for the volcano's magma plumbing system, and for improving the geodetic monitoring strategy to better anticipate the start of the next eruptive episode? Such questions can only be answered with any certainty through additional research, but here we offer a few ideas from a geodetic perspective. The sudden appearance of the 1980 north-flank bulge and 2004 crater-floor welt, neither of which seems to have been preceded by more than a minor amount of far-field deformation, suggests to us that elastic deformation of the crust surrounding the magma reservoir slows as the confining strength of the reservoir-plus-shallow-conduit system is approached. A plausible explanation for such behavior is that rock surrounding the reservoir is compressible (i.e., deforms in response to pressure changes) to a degree but becomes less so at high strain values (i.e., at high reservoir pressures). Stated differently, the host rock initially deforms elastically in response to increasing reservoir pressure but it becomes progressively more resistant ("stronger") as the strain increases. Under such circumstances, an incremental pressure increase in the reservoir produces progressively less deformation of the host rock until failure occurs. Prior to failure, pressure in the reservoir continues to increase as a result of fluid exsolution/expansion or addition of gas-rich magma from below. Magma in the reservoir is sufficiently compressible to accommodate the pressure increase without deforming the walls until a critical pressure is reached and failure occurs.

In the case of Mount St. Helens in 1980 and 2004, it seems that the first point of failure occurred above the reservoir at depths of less than 5 km below the surface, presumably along the conduit walls. Reservoir magma rose into the conduit, pushing ahead of it the conduit fill—presumably a combination of solid lava from the previous eruption and material from the conduit walls—as a relatively rigid plug to form the north-flank bulge and crater-floor welt at the surface. We imagine that the conduit fill became decoupled from the rest of the edifice to the extent that increasing pressure in the reservoir was able to force magma up the conduit without significantly deforming the broader edifice. The process is akin to a cork being pushed out of a goat skin bag that is filling with fluid. The bag inflates until its capacity is reached, whereupon inflation slows and the bag begins to pressurize. If the bag is strong enough, the cork eventually is no longer able to withstand the stress and fails. Initially, failure is incremental; this was the situation at Mount St. Helens from March 20 to May 17, 1980, and also starting on September 23, 2004. In the first case, catastrophic gravitational failure of the bulge was followed by a highly explosive eruption, i.e., the cork was blown out. In 2004, sluggish magma moving up the conduit from the crystal-rich, gas-poor top of the reservoir produced only a few brief explosions, the conduit fill (cork) was pushed ahead to the surface, and extrusion of solidified spines from the shallow reservoir and conduit continued for the next four years (Fig. 5.5).

This "strong bag–weak cork" model of the magma plumbing system at Mount St. Helens has some clear implications for designing a geodetic monitoring strategy and for adjusting expectations concerning likely precursors to the next eruptive episode. On the basis of observations and numerical models of volcano deformation, Dzurisin (2003) argued that a comprehensive geodetic monitoring network should include sensors in both proximal and distal areas, i.e., both closer than 10 km and farther than 20 km from the vent. Distal stations are especially important if the deformation source is more than 5 km deep, which is the case for the magma reservoir at Mount St. Helens. Such a broad network is appropriate to monitor surface deformation that might accompany the early stages of reservoir repressurization. Later in the eruption cycle, however, the model described above suggests that broad surface deformation might slow or cease, rendering distal monitoring stations less useful for volcano monitoring purposes (although still important to measure regional tectonic strain). At that point, it becomes important to monitor areas close to the conduit in order to detect incipient failure of the conduit plug. As was the case in 1980 and 2004, sudden onset of shallow seismicity accompanied by extreme but localized surface deformation likely will be the best short-term indicators of the next eruptive episode. Accordingly, CGPS stations have been installed on the volcano's flanks and 1980s lava dome. Incoming signals are sampled once per second (1 Hertz) and resulting phase data are streamed to the USGS Cascades Volcano Observatory, where they are processed to obtain time series of station displacements in real time—all in hopes of recognizing the next bulge or welt much earlier than was the case in 1980 or 2004.

5.3.2 Kīlauea Volcano, Hawaii

Kīlauea is among the most active and thoroughly studied volcanoes in the world. As a result, much is known about the volcano's magma storage and transport system. As is the case for Mount St. Helens, our understanding of Kīlauea's magma plumbing system is based on information from many disciplines, including seismology, geodesy, petrology, and gas geochemistry. Here we briefly describe a generalized model for Kīlauea with emphasis on what has been learned from geodetic studies. Readers interested in more detailed information about Kīlauea are encouraged to consult the original research papers cited below.

In a now-famous paper in the journal *Science*, Eaton and Murata (1960) described the structure and workings of Hawaiian volcanoes as deciphered from nearly 50 years of research at the Hawaiian Volcano Observatory, which was established in 1912 near the summit of Kīlauea by Dr. Thomas A. Jaggar (Babb et al. 2011). They sketched a cross section of an idealized Hawaiian volcano showing a magma source region at about 60 km depth, a near-vertical conduit system through the upper mantle and crust, and a shallow magma storage reservoir a few kilometers beneath the summit (Eaton and Murata 1960, p. 930). They also discussed the role played by rift zones in transporting magma laterally from the summit reservoir to vents on the volcano's flanks. Now, more than 50 years later, these basic elements remain in the modern view of Kīlauea's magma plumbing system—although much has been learned in the interim.

Tilling and Dvorak (1993, p. 126) reproduced the sketch by Eaton and Murata (1960) and provided an updated version with new information specific to Kīlauea. They noted that the paper by Eaton and Murata (1960) pre-dated the theory of plate tectonics, and that the magma source region identified by Eaton and Murata (1960) now is ascribed to the Hawaiian hotspot. On the basis of geochemical studies of Hawaiian lavas and mantle xenoliths, Tilling and Dvorak (1993) increased the depth of partial melting from about 60 to ≥80 km. They provided more detail about the nature of the magma pathway through the asthenosphere and lithosphere as illuminated by the distribution of earthquake foci and the occurrence of deep volcanic tremor. Regarding the summit magma reservoir, Tilling and Dvorak (1993) noted that analyses of geodetic surveys made after 1960 showed that pressure centers responsible for episodes of summit uplift or subsidence were located in the upper half of an aseismic zone at 2–7 km depth, i.e., the presumed shallow reservoir. Geodesy also contributed directly to two additional refinements of the Eaton and Murata (1960) model. Tilling and Dvorak (1993, p. 127) emphasized the importance of secondary magma reservoirs along Kīlauea's rift zones, which were identified on the basis of localized ground deformation and petrologic evidence. They also discussed the remarkable mobility of the volcano's south flank and its implications for magma storage along the east rift zone (Swanson et al. 1976). Details of Kīlauea's magma plumbing system, such as the amount of deep magma storage beneath the summit and rift zones (Delaney and et al. 1990; Dvorak and others, 1994), and the existence of two of more distinct reservoirs beneath the summit area (Cervelli and Miklius 2003) continue to be explored. Nonetheless, the general model described by Eaton and Murata (1960) as updated by Tilling and Dvorak (1993) remains viable.

5.3.3 Probing Aleutian Volcanoes with InSAR

None of more than 50 Aleutian volcanoes that have been active during historical time is as well studied as Mount St. Helens or Kīlauea, so the conceptual models of Aleutian volcanoes that we present in the next chapter are necessarily less detailed and more speculative—some might say fanciful—than the ones described above. At some Aleutian volcanoes, there is clear geodetic evidence for crustal magma reservoirs that fill prior to eruptions, drain during eruptions, and then are replenished as the cycle begins anew. Most of these reservoirs are located 3–10 km beneath the volcano, but in a few cases they are offset laterally by up to 10 km from the vent area. The connections between such reservoirs and the vents they feed are not well understood, but regional tectonic influences on magma migration pathways seem likely. There is abundant evidence in the Aleutians for interplay between tectonism and volcanism. In one case, magma accumulating aseismically beneath a volcano seemingly triggered a swarm of tectonic earthquakes 30 km distant. In another, a phreatic eruption at Mount Vsevidof might have been triggered by the M_L 8.6 Andreanof Islands earthquake in March 1957 (http://avo.alaska.edu/volcanoes/activity.php?volcname=Vsevidof&eruptionid=111&page=basic). There are examples of volcanoes that erupt without deforming and others that deform without erupting. InSAR can provide little insight into several historically active Aleutian volcanoes that have not deformed appreciably during the two-decade period of observation since ERS-1 was launched in 1991. In such cases we report the absence of observed deformation and present high-resolution SAR images of the volcanoes that might be useful as a baseline for studies of changing surface morphology. For volcanoes that have deformed or shown other signs of unrest (e.g., seismicity, thermal activity), we discuss representative deformation interferograms and associated source models as a basis for speculating on the configuration of the magma plumbing system. We recognize that our understanding of Aleutian volcanoes is a work in progress and that many of our ideas will be proven wrong. That said, we hope that the material presented below will serve as a useful point of departure for future studies and progress.

References

Agustsson, K., Stefansson, R., Linde, A.T., Einarsson, P., Sacks, I.S., Gudmundsson, G. B., et al. (2000) Successful prediction and warning of the 2000 eruption of Hekla based on seismicity and strain changes (abstract). *Eos, Transactions, American Geophysical Union*, *81*(48), Fall Meeting Supplement, F1337.

Anderson, E. M. (1936). The dynamics of the formation of cone-sheets, ring-dikes and cauldron-subsidences. *Proceedings Royal Society Edinburgh*, *56*, 128–157.

Babb, J. L., Kauahikaua, J. P., & Tilling, R. I. (2011) The story of the Hawaiian Volcano Observatory—a remarkable first 100 years of tracking eruptions and earthquakes. U.S. Geological Survey General Information Product 135, 60 pp., available at http://pubs.usgs.gov/gip/135/.

Battaglia, M., Gottsmann, J., Carbone, D., & Fernández, J. (2008). 4D volcano gravimetry. *Geophysics*, *73*(6), WA3–WA18. doi: 10.1190/1.2977792

Brantley, S. R., & Myers, B. (2000). Mount St. Helens from the 1980 eruption to 2000. U.S Geological Survey Fact Sheet 036-00 (http://pubs.usgs.gov/fs/2000/fs036-00/).

Caputo, M. (1979). Two thousand years of geodetic and geophysical observations in the Phlegraean Fields near Naples. *Geophysical Journal of the Royal Astronomical Society, 56*, 319–328.

Casadevall, T.J. (ed.) (1994). Volcanic ash and aviation safety: proceedings of the first international symposium on volcanic ash and aviation safety, U.S. Geological Survey Bulletin. 2047, 450 pp.

Cashman, K. V. (1988). Crystallization of Mount St. Helens dacite—a quantitative textural approach. *Bulletin of Volcanology, 50*, 194–209.

Cervelli, P., & Miklius, A. (2003). The shallow magmatic system of Kīlauea Volcano. In C. Heliker, D. A. Swanson & T. J. Takahashi (Eds.), *The Pu'u 'O'o-Kupaianaha eruption of Kīlauea Volcano, Hawai'i: the first 20 years* (pp. 149–164) U.S. Geological Survey Professional Paper 1676.

Chadwick, W. W, Jr, Swanson, D. A., Iwatsubo, E. Y., Heliker, C. C., & Leighley, T. A. (1983). Deformation monitoring at Mount St. Helens in 1981 and 1982. *Science, 221*, 1378–1380.

Chadwick, W. W., Archuleta, R. J., & Swanson, D. A. (1988). The mechanics of ground deformation precursory to dome-building extrusions at Mount St. Helens 1981–1982. *Journal of Geophysical Research, 93*, 4351–4366.

Chouet, B. (2003). Volcano seismology. *Pure and Applied Geophysics, 160*, 739–788.

Christiansen, R. L., & Peterson, D. W. (1981). Chronology of the 1980 eruptive activity. In P. W. Lipman, & D. R. Mullineaux (Eds.), *The 1980 eruptions of Mount St. Helens, Washington* (pp. 17–30). U.S. Geological Survey Professional Paper 1250.

Delaney, P. T., Fiske, R. S., Miklius, A., Okamura, A. T., & Sako, M. K. (1990). Deep magma body beneath the summit and rift zones of Kīlauea Volcano, Hawaii. *Science, 247*, 1311–1316.

Dvorak, J. J., Klein, F. W., & Swanson, D. A. (1994). Relaxation of the south flank after the 7.2-magnitude Kalapana earthquake, Kīlauea Volcano, Hawaii. *Bulletin of the Seismological Society of America, 84*(1), 133–141.

Dzurisin, D. (2000). Volcano geodesy—challenges and opportunities for the 21st century. *Philosophical Transactions of the Royal Society, London, Series A, 358*, 1547–1566.

Dzurisin, D. (2003). A comprehensive approach to monitoring volcano deformation as a window on eruption cycle. *Reviews of Geophysics, 41*, 1–29. doi:10.1029/2001RG000107.

Dzurisin, D., Westphal, J. A., & Johnson, D. J. (1983). Eruption prediction aided by electronic tiltmeter data at Mount St. Helens. *Science, 221*, 1381–1383.

Dzurisin, D., Lisowski, M., Poland, M. P., Sherrod, D. R., & LaHusen, R. G. (2008). Constraints and conundrums resulting from ground-deformation measurements made during the 2004–2005 dome-building eruption of Mount St. Helens, Washington. In D. R. Sherrod, W. E. Scott & P. H. Stauffer (Eds.), *A volcano rekindled—the renewed eruption of Mount St. Helens, 2004–2006* (pp. 281–300). U.S. Geological Survey Professional Paper 1750.

Eaton, J. P., & Murata, K. J. (1960). How volcanoes grow. *Science, 132*(3432), 925–938.

Endo, E. T., Malone, S. D., Noson, L. L., & Weaver, C. S. (1981). Locations, mgnitudes, and satistics of the March 20–May 18 earthquake sequence. In P. W. Lipman, & D. R. Mullineaux (Eds.), *The 1980 Eruptions of Mount St. Helens, Washington* (pp. 93–107). U.S. Geological Survey Professional Paper 1250.

Ewert, J.,& Swanson, D. A. (Eds.) (1992). Monitoring volcanoes—techniques and strategies used by the staff of the Cascades Volcano Observatory, 1980–90. U.S. Geological Survey Bulletin 1966, 223 pp.

Gerlach, T. M., McGee, K. A., Elias, T., Sutton, A. J., & Doukas, M. P., (2002). Carbon dioxide emission rate of Kīlauea Volcano—implications for primary magma and the summit reservoir. *Journal of Geophysical Research*, *107*(B9), 2189. doi: 10.1029/2001JB000407

Husen, S., Smith, R. B., & Waite, G. P. (2004). Evidence for gas and magmatic sources beneath the Yellowstone volcanic field from seismic tomographic imaging. *Journal of Volcanology and Geothermal Research, 131*, 397–410.

Linde, A. T., Agustsson, K., Sacks, I. S., & Stefansson, R. (1993). Mechanism of the 1991 eruption of Hekla from continuous borehole strain monitoring. *Nature, 365*, 737–740.

Lipman, P. W., Moore, J. G., & Swanson, D. A. (1981). Bulging of the north flank before the May 18 eruption—geodetic data. In P. W. Lipman, & D. R. Mullineaux (Eds.), *The 1980 eruptions of Mount St. Helens, Washington* (pp. 143–155). U.S. Geological Survey Professional Paper 1250.

Lisowski, M. (2007) Analytical deformation source models. In D. Dzurisin (Ed.), *Volcano deformation—geodetic monitoring techniques* (pp. 279–304). Berlin: Springer.

Lisowski, M., Dzurisin, D., Denlinger, R. P., & Iwatsubo, E. Y. (2008). Analysis of GPS-measured deformation associated with the 2004–2006 dome-building eruption of Mount St. Helens, Washington. In D. R. Sherrod, W. E. Scott & P. H. Stauffer (Eds.), *A volcano rekindled—the renewed eruption of Mount St. Helens, 2004–2006* (pp. 301–333). U.S. Geological Survey Professional Paper 1750.

Malone, S. D., Endo, E. T., Weaver, C. S., & Ramey, J. W. (1981). Seismic monitoring for eruption prediction. In P. W. Lipman, & D. R. Mullineaux (Eds.), *The 1980 eruptions of Mount St. Helens, Washington* (pp. 803–813). U.S. Geological Survey Professional Paper 1250.

Mastin, L. G., Roeloffs, E., Beeler, N. M., & Quick, J. E. (2008) Constraints on the size, overpressure, and volatile content of the Mount St. Helens magma system from geodetic and dome-growth measurements during the 2004–2006 + eruption. In D. R. Sherrod, W. E. Scott & P. H. Stauffer (Eds.), *A volcano rekindled—the renewed eruption of Mount St. Helens, 2004–2006* (pp. 461–488). U.S. Geological Survey Professional Paper 1750.

McCann, G. D., & Wilts, C.H. (1951). *A mathematical analysis of the subsidence in the Long Beach–San Pedro Area.* Pasadena, USA: Internal Report, California Institute of Technology.

Mogi, K. (1958). Relations between the eruptions of various volcanoes and the deformation of the ground surfaces around them. *Bulletin of the Earthquake Research Institute, University of Tokyo, 36*, 99–134.

Moran, S. C., (1994). Seismicity at Mount St. Helens, 1987 to 1992—evidence for repressurization of an active magmatic system. *Journal of Geophysical Research*, *99*(B3), 4341–4354. doi: 10.1029/93JB02993

Moran, S. C., Malone, S. D., Qamar, A. I., Thelen, W. A., Wright, A. K., & Caplan-Auerbach, J. (2008). Seismicity associated with renewed dome building at Mount St. Helens, 2004–2005. In D. R. Sherrod, W. E. Scott & P. H. Stauffer (Eds.), *A volcano rekindled—the renewed eruption of Mount St. Helens, 2004–2006* (pp. 27–60). U.S. Geological Survey Professional Paper 1750.

Mullineaux, D. R. (1996). *Pre-1980 tephra-fall deposits erupted from Mount St. Helens, Washington*. U.S. Geological Survey Professional Paper 1563, 99 pp.

Newhall, C. G., & Dzurisin, D. (1988) *Historical unrest at large calderas of the world*. U.S. Geological Survey Bulletin 1855, 1108 pp.

Oppenheimer, C., Francis, P., Burton, M., Maciejewski, A. J. H., & Boardman, L. (1998). Remote measurement of volcanic gases by Fourier transform infrared spectroscopy. *Applied Physics B, 67*, 505–515.

Pallister, J. S., Hoblitt, R. P., Crandell, D. R., & Mullineaux, D. R. (1992). Mount St. Helens a decade after the 1980 eruptions—magmatic models, chemical cycles, and a revised hazards assessment. *Bulletin of Volcanology, 54*, 126–146.

Pallister, J.S., Thornber, C. R., Cashman, K. V., Clynne, M. A., Lowers, H. A., Mandeville, C. W., Brownfield, I. K., & Meeker, G. P. (2008). Petrology of the 2004–2006 Mount St. Helens lava dome—implications for magmatic plumbing and eruption triggering. In D. R. Sherrod, W. E. Scott & P. H. Stauffer (Eds.), *A volcano rekindled—the renewed eruption of Mount St. Helens, 2004–2006* (pp. 647–702) U.S. Geological Survey Professional Paper 1750.

Parascandola, A. (1947). *I fenomeni bradisismici del Serapeo di Pozzuoli. Napoli: Stabilimento Tipografico G. Genovese* (p. 156) (M. Capuano & J. Dvorak, Trans.).

Roeloffs, E. A., & Linde, A. T., (2007). Borehole observations of continuous strain and fluid pressure. *Volcano deformation—geodetic monitoring techniques* (pp. 305–322). Berlin: Springer.

Scandone, R., & Malone, S. D. (1985). Magma supply, magma discharge and readjustment of the feeding system of Mount St. Helens during 1980. *Journal of Volcanology and Geothermal Research, 23*, 239–262.

Schilling, S. P., Thompson, R. A., Messerich, J. A., & Iwatsubo, E. Y. (2008). Use of digital aerophotogrammetry to determine rates of lava dome growth, Mount St. Helens, Washington, 2004–2005. In D. R. Sherrod, W. E. Scott & P. H. Stauffer (Eds.), *A volcano rekindled—the renewed eruption of Mount St. Helens, 2004–2006* (pp. 145–167). U.S. Geological Survey Professional Paper 1750.

Scott, W. E., Sherrod, D. R., & Gardner, C. A. (2008). Overview of the 2004–2006, and continuing, eruption of Mount St. Helens, Washington. In D. R. Sherrod, W. E. Scott & P. H. Stauffer (Eds.), *A volcano rekindled—the renewed eruption of Mount St. Helens, 2004–2006* (pp. 3–22). U.S. Geological Survey Professional Paper 1750.

Sutton, A. J., McGee, K. A., Casadevall, T. J., & Stokes, J. B. (1992). Fundamental volcano-gas-study techniques—an integrated approach to monitoring. In J. Ewert & D. A. Swanson (Eds.), *Monitoring volcanoes—techniques and strategies used by the staff of the Cascades Volcano Observatory 1980–90* (pp. 181–188). U.S. Geological Survey Bulletin 1966

Swanson, D. A., Duffield, W. A., & Fiske, R. S. (1976). Displacement of the south flank of Kīlauea volcano—the result of forceful intrusion of magma into the rift zones. U.S. Geological Survey Professional Paper 963, 39 pp.

Swanson, D. A., Casadevall, T. J., Dzurisin, D., Malone, S. D., Newhall, C. G., & Weaver, C. S. (1983). Predicting eruptions at Mount St. Helens, June 1980 through December 1982. *Science, 221*, 1369–1376.

Swanson, D. A., Dzurisin, D., Holcomb, R. T., Iwatsubo, E. Y., Chadwick, W. W, Jr, Casadevall, T. J., et al. (1987). Growth of the lava dome at Mount St. Helens, Washington (USA), 1981–83. In J. H. Fink (Ed.), *Emplacement of silicic domes and lava flows* (pp. 1–16). Boulder: Geological Society of America. Geological Society of America Special Paper 212.

Tilling, R. I., & Dvorak, J. J. (1993). Anatomy of a basaltic volcano—Kīlauea, Hawaii. *Nature, 363*, 125–133.

Vallance, J. W., Schneider, D. J., & Schilling, S. P. (2008). Growth of the 2004–2006 lava-dome complex at Mount St. Helens, Washington, In D. R. Sherrod, W. E. Scott & P. H. Stauffer (Eds.), *A volcano rekindled—the renewed eruption of Mount St. Helens, 2004–2006* (pp. 169–208). U.S. Geological Survey Professional Paper 1750.

Waite, G.P., & Moran, S.C., (2009). Vp structure of Mount St. Helens, Washington, USA, imaged with local earthquake tomography. *Journal of Volcanology and Geothermal Research*, *182*(1-2), 113–122.

Weaver, C. S., & Smith, S. W. (1983). Regional tectonic and earthquake hazard implications of a crustal fault zone in southwestern Washington. *Journal of Geophysical Research*, *88*(B12), 10371–10383.

Weaver, C. S., Grant, W. C., Malone, S. D., & Endo, E. T. (1981). Post-May 18 seismicity: Volcanic and tectonic implications. In P. W. Lipman, & D. R. Mullineaux (Eds.), *The 1980 Eruptions of Mount St. Helens, Washington* (pp. 109–121). U.S. Geological Survey Professional Paper 1250.

Yamakawa, N. (1955). On the strain produced on a semi-infinite elastic solid by an interior source of stress. *Journal of the Seismological Society of Japan, 8*, 84–98.